Very large differences in intramolecular D-H partitioning in hydrated silicate melts synthesized at upper mantle pressures and temperatures [Revision 1]

Ying Wang, Samantha X. Cody, Dionysis Foustoukos,

Bjorn O. Mysen, George D. Cody*

Geophysical Laboratory, Carnegie Institution of Washington

Corresponding Author Contact Information: George D. Cody Geophysical Laboratory, Carnegie Insitution of Washington, 5251 Broad Branch Rd., NW, Washington, DC 20015, gcody@ciw.edu

Abstract

Hydrated (with D_2O and H_2O) sodium tetrasilicate glasses, quenched from melts at 1400˚C and 1.5 GPa, are studied using ^{1}H, ^{2}H and ^{29}Si solid state Nuclear Magnetic Resonance (NMR) Spectroscopy. Whereas D_2O and H_2O depolymerize the silicate melt to similar degrees, protium and deuterium intramolecular partitioning between different molecular sites within the glasses is very different and exemplified by a strong preferential association of deuterons to sites with short O-D•••O distances. This preference is independent of total water content and D/H ratio. Substantially different intramolecular D-H partitioning is also observed in a glass with a model hydrous basalt

composition. Such large differences in isotope partitioning cannot result from classic equilibrium fractionation because of the high synthesis temperature. Potential kinetic isotope effects are excluded via a slow quench experiment. The apparent fractionation is likely governed by density/molar volume isotope effects, where deuterium prefers sites with smaller molar volume. Large diffences in intramolecular site partitioning in melts could lead to significant differences in D-H partitioning between water saturated melt and exsolved aqueous fluid (where $D/H_{W,Melt} \neq D/H_{W,Fluid}$) during crystallization of Earth's magma ocean, potentially controlling the D/H content of the Earth's oceans.

Keywords. Hydrogen Isotopes, Silicate Melts, fractionation

Introduction

Hydrogen isotope fractionation during magmatic processes is key to understanding the deep Earth hydrological cycle and may place constraints on the origin of Earth's oceans. It is well established that the D/H content of water in hydrated nominally anhydrous mantle minerals is systematically lower (< -100 ‰) than the standard mean ocean water (SMOW, D/H = 1.5576×10^{-4}, defined as 0 ‰) (Bell and Ihinger, 2000). Experiments have revealed significant hydrogen isotope partitioning between melts and fluids or vapors at magmatic temperatures (e.g. Kuroda et al. 1982; Richet et al. 1986; Dobsen et al. 1989; Pineau et al. 1998; Mysen 2013). The origin of such fractionation, given the high temperatures of magmatic processes, is not likely due to equilibrium isotope effects as described by statistical mechanics (Urey 1947; Bigeleisen and Mayer 1947).

Near Infrared (NIR) spectroscopy reveals that water exists in quenched melts as hydroxyl (silanol) and molecular water (Stolper 1982); where the proportion of these species is a function of water concentration and temperature (Nowak and Behrens 1995). The possibility that fractionation of hydrogen isotopes exists between silanol and molecular water within melts has been considered (Dobsen et al. 1989). Whereas NIR spectroscopy reveals distinct bands for silanol and molecular water, the primary O-H vibrational structure in the mid-infrared region cannot distinquish been these primary species (Zotov and Keppler, 1998). What is observed in the mid Infrared region with hydrous glasses at room temperature is very complex vibrational structure spanning a very wide frequency range. Interestingly, a FTIR study comparing primary O-H and O-D vibrational structure in a hydrated (with H_2O and D_2O) sodium tetrasilicate glasses, does suggest differences in the intensities of various OH and OD vibrational modes (Zotov and Keppler, 1998), possibly indicating differences in intramolecular D-H partitioning between different molecular sites within the hydrated silicate glass. However, in the study of Zotov and Keppler (1998) the deuterated and hydrated glasses were separately prepared samples, thus the apparent differences in vibrational intensities across the mid-infrared could be attributed to slight differences in water composition or synthesis conditions across the two samples.

Solid state ^{1}H Nuclear Magnetic Resonance (NMR) spectroscopy is a powerful tool for the study of water in hydrous silicate glasses quenched from melts. Previous studies have shown that water resides in wide range of molecular environments within glasses formed in this manner (e.g. Eckert et al. 1987, 1988; Kohn et al. 1989; Schaller and Sebald 1995; Cody et al. 2005; Xue and Kanzaki 2009). The ^{1}H solid state NMR

spectrum of silanol and water in hydrous glasses is understood to be predominantly controlled by O-H•••O distance (Eckert et al. 1988, Xue and Kanzaki 2001). Similar to mid IR vibrational spectroscopy, ^{1}H solid state NMR cannot readily distinguish between silanol and molecular water, i.e., hydrogen's chemical shift is unaffected by whether the oxygen it is bonded to is water or a siloxy group.

Solid state NMR does have the advantage that it is an isotope specific emission spectroscopy, therefore, signal interference between different isotopes is very rarely a problem and one can investigate mixed isotopic systems without interference. In the present study ^{1}H, ^{2}H and ^{29}Si solid-state Nuclear Magnetic Resonance (NMR) spectroscopy was performed on hydrated sodium tretrasilicate glasses quenched from melt, at various water contents and variable D/H content. ^{1}H and ^{2}H solid state NMR were also performed on a hydrous glass with a model basalt composition. We show that large differences in intramolecular H-D partitioning are evident in all of the glasses studied.

Methods and Analytical Techniques

Sample preparation

This study employed two types of glasses: a hydrated sodium tetrasilicate ($Na_2O{\cdot}4SiO_2$, hereafter referred to as NS4) glass, which is a classic model system investigated by multiple techniques (e.g. Schaller and Sebald 1995; Kummerlin et al 1992; Zotov and Keppler, 1998) and a synthetic, iron-free, hydrated glass of basalt-like composition ($10CaO{\cdot}20MgO{\cdot}5Na_2O{\cdot}15Al_2O_3{\cdot}50SiO_2$, hereafter referred to as CMNAS). The starting dry NS4 glass was made by mixing spectroscopically pure Na_2CO_3 and SiO_2, ground under alcohol for ~ 1 h, and then decarbonated during slow heating

(~1.5°C/min). The resultant mixture was melted at ambient pressure in a Deltech furnace in open Pt crucibles at 1500°C for 60 min and then quenched to glass. The dry CMNAS glass was similarly synthesized with a melting temperature of 1400°C. These anhydrous starting glasses were crushed to ≥ 20 μm grains and stored at 110°C when not used.

To prepare for the synthesis of hydrous glasses, pure D_2O (99.5%) was mixed with isotopically unlabeled distilled deionized water at desired ratios to produce a series of solutions with D abundance varying from 0 to 100% (Table 1). Water was injected into Pt capsules, approximately 5 mm O.D. × 10 mm long, using a 10-μL microsyringe. The anhydrous glasses were then added to the same Pt capsules which were welded shut using a tungsten inert gas high frequency pulsed arc welder (Lampert PUK 3S). The use of a pulsed arc welder greatly reduces the heating and potential for water loss during welding. The exact amount of H_2O added was determined by weight. The average total sample mass (water + anhydrous glass) was around ~ 200 mg. The weighing accuracy was ± 0.02 mg, which gives accuracy < ± 0.1% in the reported water contents. Table 1 summarizes the water content and hydrogen isotopic composition of all the glasses synthesized in this study.

The sealed Pt capsules containing the starting glass and water were loaded in 0.75-diameter furnace assemblies and then subjected to high-pressure (1.5 GPa) and high-temperature (1400°C) experiments in a solid-media, high-pressure apparatus. Temperatures were measured with Pt-$Pt_{90}Rh_{10}$ thermocouples. The estimated uncertainties are ±10°C and ± 0.1 GPa, respectively. The experimental temperature was programmed to initially rise from room temperature to 1400 °C at 300 °C /sec. The duration of each run was 3+ hrs, followed by quenching to glass at a rate of 100˚C/s.

In order to test for potential kinetic isotope effects, one sample was also subjected to prolonged heating at 1.5 GPa for 48 hours to test for the attainment of D-H equilibrium (Table 1). This run was then quenched slowly at 1 °C/min in order to see whether H and D partitioning changed relative to the standard experiment, as a test for potential mass-derived kinetic isotope effects that might occur during any re-equilibration upon cooling to the glass transition temperature (see discussion in section 3.3). For comparison with hydrogen speciation in various glasses and minerals, we also prepared two hydrous SiO_2 glasses containing either 14 mol% H_2O or D_2O for ^{1}H and ^{2}H NMR analysis. Also included for comparison is a sample of natural gypsum ($CaSO_4 \bullet 2H_2O$).

^{29}Si, ^{1}H, and ^{2}H solid state NMR spectroscopy

NMR experiments were performed with a Varian-Chemagnetics Infinity 300 solid-state NMR spectrometer with a static field of ~7.05 T. The resonance frequencies of ^{1}H, ^{2}H, and ^{29}Si nuclei are 300, 46, and 59 mHz, respectively. ^{1}H and ^{29}Si spectra were referenced to tetramethylsilane (TMS), while ^{2}H spectra were referenced to perdeuterated-tetramethylsilane (TMS-$^{2}H_{12}$, 99%, from C/D/N Isotopes).

The ^{1}H NMR spectra were obtained by ^{1}H single-pulse magic-angle-spinning (MAS) experiments employing a 2.5 mm rotor and fast MAS probe with spinning frequency ($\omega_r/2\pi$) of 22 kHz. The DEPTH four pulse sequence was employed to suppress background ^{1}H signal where phase cycling (n=16) removes any signal from background protons (outside the RF coil) that experience a nutation angle of less than 45 °. The acquisition parameters include a ^{1}H 90° RF pulse length of 3 μs, a recycle delay

of 100 s (the spin-latice relaxation time, T_1, for ^1H in these glasses was determined by experiment to be 20 s) and a spectral width of 200 kHz. A total of 1600 acquisitions were acquired per sample.

The ^2H NMR spectra were obtained by ^2H single pulse experiments at MAS frequency of 8 kHz (controlled to ± 1 Hz). The ^2H excitation pulse width was 1.5 μs ($\omega_1/2\pi$ = 55.5 kHz) corresponding to a 30 °C nutation angle. Spinning at this rate is sufficient to induce complete homonuclear decoupling and significantly average out much of the ^1H-^2H coupling. In order to ensure complete ^1H-^2H decoupling, high power ^1H decoupling was performed during signal acquisition with $\omega_1/2\pi$ = 62.5 KHz. A pulse delay of 10 s was employed to minimize interference due to longitudinal (spin-lattice) relaxation effects [previous estimates of ^2H's T_1 in silicate glasses was less than 1 s (Ekert et al. 1987)]. A total of 16000 acquisitions were acquired per sample.

^2H is a spin-1 quadrupole and static NMR spectra of ^2H in a rigid solid yields a classic Pake powder pattern spectrum spanning a spectral width that is dependent on the strength of the quadrupolar interaction, in some cases in excess of 200 kHz for ^2H in rigid environments (Eckert et al. 1987). Under fast MAS rotation the quadrupolar powder pattern is defined by multiple spinning sidebands that spread out over the frequency range of quadrupole interaction. While it is possible to fit all of the side bands in order to obtain the site specific powder patterns to quantify the standard ^2H MAS NMR spectra, an alternative approach provides purely isotropic ^2H MAS NMR spectra that are more directly comparable to ^1H MAS NMR spectra. Isotropic spectra were obtained by rotor synchronized acquisition, where the spectral width is exactly equal to the MAS frequency (8 KHz ± 1 Hz), thus the dwell is equal to the rotor period.

The receiver band width was set at 600 KHz, thus all of the sidebands detected outside of the spectral window are perfectly aliased into the central band, greatly increasing the signal-to-noise ratio and yielding a purely isotropic spectrum (see for example Eckman, 1982; Ashbrook and Wimperis, 2005).

Given that the ^{2}H quadrupolar interaction may be 200 kHz or larger and given that the maximum power of the RF pulse is 55.5 kHz suggests that off resonance effects may be expected (Ernst et al. 1991). In the case where ^{2}H in different environments have significanly different quadrupolar interaction strengths, ^{2}H with larger quadrupolar interactions could have suppressed signal intensity in the rotationally resonant isotropic spectrum (Eckman, 1982). Consideration of the potential of such artifacts are addressed in the discussion below. In one case, wide line ^{2}H MAS NMR was acquired, where the spectral width was 600 kHz and the nutation time was 500 ns to minimize off resonance effects.

Single pulse ^{29}Si NMR spectra were obtained with MAS frequency of 8 kHz, ^{29}Si pulse widths corresponding to 30° tip angles, a recycle delay of 100 s, and co-addition of 1000 acquisitions. Proton decoupling was performed with continuous RF irradiation at 62.5 kHz. More details on the ^{29}Si Single pulse NMR experiments can be found in (Cody et al., 2005).

Results

^{29}Si MAS NMR of hydrous (H_2O and D_2O) Sodium tetrasilicate glasses

Chemically, D_2O and H_2O are expected to interact with the sodium silicate melt similarly, i.e., both D_2O and H_2O should depolymerize the silicate network to essentially the same extent. This is confirmed with ^{29}Si solid state NMR of sodium silicate glass with 9 wt % water (Fig. 1), from which it is determined that hydrogen exists nearly equally as $(H,D)_2O$ and as silanol OH,D independent of the D-H content of water. The only means for determining the proportion of Si-OH and H_2O in NS4 glass quenched from melt via NMR is through the determination of the proportion of Q species via ^{29}Si NMR. Individual Q^n species Q^{4-0} in simple sodium tetrasilicate glasses are resolvable using ^{29}Si NMR (Maekawa et al. 1991, Kümmerlin et al. 1992, Zotov and Keppler 1998, Cody et al. 2005). Compositionally, $Q^4 = SiO_2$, $Q^3 = NaSiO_{2.5}$, and anhydrous NS4 glass $= Na_{0.5}SiO_{2.25}$; therefore, NS4 glass is expected to be composed of equal concentrations of Q^4 and Q^3, with the number of non-bridging oxygens per tetrahedron (NBO/T) being 0.5. The accuracy of determination of the proportion of Q species is clearly subject to the choice of fitting parameters, i.e., peak shape characteristics (Zotov and Keppler, 1998). In the present case the ^{29}Si spectra were fit with purely Gaussian bands with fixed peak widths where Q^4 is centered at -103 ppm, Q^3 at -95 ppm, and Q^2 at -90 ppm. The resulting percentages of Q^4, Q^3, and Q^2 are presented in Table 2. Whereas anhydrous NS4 glass has an NBO/T of 0.5, NS4 glass with 9 wt % water in the form of H_2O, D_2O or mixed H_2O-D_2O has an NBO/T of 0.88-0.92 that is expectedly independent of the D-H composition of the water. The increase in NBO/T with water addition reflects the additional depolymerization of the silicate oxide network by water, where Na_2O is expected to act only as a depolymerizing agent, and the speciation of water between Si-OH and H_2O is readily attained (Table 2). This degree of depolymerization

is in accord with other data at this water content (Stolper, 1982, Zotov and Keppler, 1998); where differences are ascribed to the approach to fitting (Kümmerlen et al. 1992; Zotov and Keppler 1998; Cody et al. 2005).

^{1}H and ^{2}H MAS NMR of hydrous sodium tetrasilicate glasses

The ^{1}H MAS NMR spectrum of sodium tetrasilicate glass (NS4) is complex (Fig. 1, center), spanning a wide range of frequencies, but with intensity concentrated in a low to intermediate-frequency band spanning from 0 up to 7 ppm and an asymmetric high-frequency band extending out to 16 ppm. These bands are clearly composite bands of numerous overlapping resonances based on their asymmetric peak shapes. For comparison, ^{1}H NMR of $CaSO_4$•$2H_2O$ (gypsum) and water containing SiO_2 glass, quenched from melt are also shown. The molecular H_2O in gypsum gives rise to a broad symmetric resonance at 5.5 ppm, whereas hydrated SiO_2 melt quenched to glass exhibits a sharp resonance nearly coincident with a broader peak, at 4.9 and 5.6 ppm, respectively. Focusing on the hydrous NS4 glass (Fig. 1, center), the high-frequency ^{1}H resonance band at 16 ppm corresponds to a particularly short O-H•••O distances (Eckert et al. 1988, Xue and Kanzaki 2001). The low to intermediate frequency resonance band at ~ 5 ppm corresponds to water and silanol residing in sites with longer O-H•••O distances (Fig. 1, center). Evidently one result of network depolymerization upon Na_2O addition to SiO_2 is the creation of sites for OH and H_2O with short O-H•••O distances.

The isotropic ^{2}H solid state NMR spectra is expected to be very similar to that of the ^{1}H solid state NMR spectra. Thus, in the case of ^{2}H in hydrated NS4 glass (Fig. 1,

right) we observe resonance intensity spanning a wide frequency range, concentrated in low and high frequency resonance bands as is observed in the ^{1}H NMR spectra of hydrated NS4 (Fig. 1, center). What is immediately obvious is that the spectral intensity distribution in the ^{1}H and ^{2}H spectra of the hydrated NS4 glasses is very different. Deuterium (^{2}H) preferentially resides in high spectral frequency sites with short O-D•••O distances, whereas hydrogen (^{1}H) populates the intermediate and high frequency regions of the spectrum nearly equally (Fig 1, center). In comparison, in the case of a pure SiO_2 melt with D_2O, quenched to glass, the ^{2}H NMR spectrum extends only to the intermediate frequency resonance bands, similar to the ^{1}H NMR spectrum of SiO_2 glass with H_2O.

This very large difference in intensity between ^{1}H and ^{2}H NMR spectra in the high and medium frequency sites was not expected. A valid concern is that the difference in intensity may result from an artifact related to the deuteron's quadrupolar interaction influencing the rotor synchronized isotropic ^{2}H spectra. In general, an ideal NMR experiment employs RF excitation pulse strength greater than any of the internal NMR interactions, e.g., the chemical shielding interaction. In the case of deuterium solid state NMR, whereas the chemical shielding interaction is relatively weak, the quadrupolar interaction is not inconsequential and is typically larger than available RF pulse power. In cases where the NMR spectrum is wider than the available RF power, off resonance effects at some level are inevitable (Ernst et al. 1991) leading to phase and amplitude errors particularly with long pulse widths (e.g. 90 ° pulses with typical RF pulse power).

It is well established that ^{1}H NMR frequency correlates with O-H•••O length (Eckert et al. 1988, Xue and Kanzaki 2001). There is also a strong correlation between O-D•••O length and the ^{2}H quadrupolar coupling constant, C_q, for that site (Ekert et al. 1987). Thus, one can corelate ^{1}H NMR frequency for a given site to ^{2}H's C_q. For the high frequency ^{1}H peak at 16 ppm (Fig. 1) one predicts a ^{2}H C_q of 113 KHz and for the intermediate frequency peak at 5 ppm one predicts a ^{2}H C_q of 240 KHz (Eckert et al. 1987). Note that these predictions assume that the deuterium atom is immobile, however, Eckert et al. (1987) showed in their study of hydrated rhyolite glass that many deuterons are partially mobile at room temperature, where motion of the deuteron has a short correlation time ($\tau_c^{-1} > C_q$). Such motion strongly effects the ^{2}H NMR spectrum by greatly reducing the spectral width (Schmidt-Rohr and Speiss, 1994). As will be shown below, non rigid deuterons are also present in these hydrated NS4 glasses.

The worse case scenario associated with off resonance effects would be spectral distortion in the isotropic ^{2}H NMR spectrum assuming rigid deuterons with C_q's of 113 and 240 KHz, corresponding to the 16 and 5 ppm sites, respectively. The net effect could be to potentially lose intensity at the 5 ppm site in the ^{2}H NMR spectrum relative to that in the ^{1}H NMR spectrum (fig. 1). The magnitude of this off resonance distortion will increase with excitation pulse width (Ernst et al. 1991). In the present experiments a pulse width of 1.5 μs, corresponding to 30 ° pulse, was employed. Such a short pulse width will help minimize off resonance distortion between ^{2}H sites with significantly different C_q's. In order to determine the magnitude, if any, of spectral distortion, assuming this worse case scenario, rotor synchronized ^{2}H MAS NMR was simulated numerically using the SIMPSON code (Bak et al. 2000) with the experimental

parameters outlined in the methods section. These calculations reveal that off resonance effects can result in the large C_q site (low frequency) exhibiting a reduction in intensity of 8 % relative to the low C_q site (high frequency). Therefore, this worse case scenario involving off resonance effects is not sufficient to explain the very large observed differences in spectral intensity distribution between ^1H and ^2H in hydrated NS4 glasses (Fig 1).

Having established that the large differences in intramolecular D-H partioning are real, hydrated NS4 glasses were synthesized from melts equilibrated with 3, 6, and 9 wt % water with pure H_2O, D_2O and mixed D-H water. From near IR studies (e.g. Stolper 1982; Nowak and Behrens 1995; Zotov and Keppler 1998) it is expected that at 3 wt % water content the dominant species is silanol (Si-OH,D), whereas at 6 wt % water, silanol and molecular water are near equal in abundance, and at 9 wt % molecular water is expected to be predominant. It is clear in Fig.s 2-4, that there are no systematic spectral trends attributable to water or D-H content. This means that whether hydrogen species are predominantly Si-OH (at 3 wt %) or majority H_2O (at 9 wt %) such speciation is not obvious in either the ^1H and ^2H MAS NMR spectra and the site affinity difference exhibited by D and H is independent of water content and D-H content. Recall that the H or D NMR frequency is not sensitive to whether either isotope is bonded to Si-OX or X_2O (X= H or D), but is sensitive to O-H•••O distance (Eckert at al. 1988, Xue and Kanzaki 2001).

In order to quantify a site affinity ratio for D and H in different regions of the ^1H and ^2H MAS NMR spectra, the relevant spectral regions need to be integrated. It is obvious from the line shapes in the ^1H and ^2H MAS NMR spectra that if one chose to fit

either spectra with Gaussian, Lorenztian, or mixed Gaussian/Lorenztian, many overlapping peaks would be required with minimal constraint on peak shape characteristics. As the point of this analysis is purely to see whether there was any trend in the partitioning ratio for D-H in between the high frequency and low frequency regions of the spectrum we chose to define the low frequency domain as the spectral area spanning from -30 ppm to 7.3 ppm (for ^{2}H MAS NMR) and -15 to 10 ppm (for ^{1}H MAS NMR) and the high frequency domain spanning the area from 7.3 ppm up to 40 ppm (for ^{2}H MAS NMR) and 10 to 30 ppm (^{1}H MAS NMR). The small differences in frequency ranges reflect the more Lorenztian shape of the ^{2}H NMR spectrum and the observation that the ^{2}H NMR spectrum is consistently shifted by ~ 2 ppm to lower frequency, relative to the ^{1}H NMR spectrum.

The integrated ^{1}H and ^{2}H NMR spectra allow quantification of the percentage of H or D residing in low and high frequency regions of the spectra, as is presented as histograms in Figure 5. While there is some variation in speciation amongst various environments exhibited by both protium and deuterium, there is no correlation with water abundance. Furthermore, the environmental partitioning of deuterons and protons within the quenched melts is independent of D/H ratio and water content.

The site affinities of deuterons and protons for the different environments responsible for the high and low frequency resonances may be quantified through a D-H partitioning factor, R, defined as $R = (D/H)_{HF}/(D/H)_{LF}$, where "HF" is the ratio of ^{2}H signal intensity in the high frequency region of the spectrum relative to ^{1}H and where "LF" is the ratio of intensity of ^{2}H intensity in the low to middle frequency region of the spectrum relative to ^{1}H. R, so defined, is determined to be very large with an average of

322 3.1 (± 0.5) reflecting the strong association of deuterium to sites with short O-D•••O
323 distances in the silicate melt (fig. 5). There is no correlation between R and the water or
324 D-H content of the glass.
325
326 **Testing for kinetic isotope effects during quenching**
327
328 The structure of these glasses is that of their melt at the glass transition where the
329 glass transition temperature is on the order of 550 to 600 °C (Mysen and Richet 2005).
330 It is known that the speciation of Si-OH and H_2O are dependent on water content
331 (Stolper, 1982; Zotov and Keppler, 1998) and temperature (Nowak and Behrens, 1995).
332 Although no evidence was found for water speciation affecting the affinity ratio (Figs 2-
333 5), there remains the possibility that kinetic isotope effects during quenching may result
334 in the observed differential partitioning. During a typical experiment, run times were
335 on the order of 3 hours and the quench rate following the run was 100 °C/second. As
336 the glass transition of hydrous NS4 melt (quenched at these rates) is on the order of 500
337 to 600 °C, 8 to 9 seconds are available for kinetic isotope effects to potentially arise
338 from mass differences in isotope diffusion rates.
339 For example, if at high temperatures, both H and D equally favor the high
340 frequency sites (shorter O-H•••O distance) but at lower temperatures favored
341 environments with longer O-H•••O distances, then if H diffusion rates were greater than
342 D, then it is possible that the apparent partitioning observed in Figs 1-5 could be due to a
343 kinetic isotope effect. To test this possibility a run was performed where the melt was
344 held at 1400 °C and 1.5 GPa for 48 hours and then quenched at a rate of 1 °C/second

(providing ca. 800 seconds for any site exchange that might occur during cooling). No change in the observed intramolecular H-D partitioning was observed (Fig. 6) relative to the fast quench samples (Fig 1-4). Integration of the ^{1}H and ^{2}H MAS NMR spectra from the slow quenched sample yielded an R of 3.1 (consistent with the fast quench samples, Fig. 5). This experiment indicates that the very large intramolecular partitioning observed with hydrated NS4 glass quenched from melts is not due to a kinetic isotope effect associated with quench rate.

Wide line ^{2}H NMR of hydrated NS4 glass: insight from quadrupolar powder patterns

Whereas the rotor synchronized ^{2}H MAS NMR spectra provide isotropic spectra directly comparable to ^{1}H MAS NMR spectra, information derived from the quadrupolar interaction is lost. Acquisition of the wide line ^{2}H MAS NMR spectrum (spectral width 600 kHz at 8 kHz MAS) reveals a broad spectrum spanning just over 200 kHz composed of 30 peaks that are spinning sidebands derived by the quadrupolar interaction, where the intensity of the sidebands trace out the static quadrupolar line shape. In Fig. 7 A & B the center band (Fig. 7A) and the most intense high frequency echo (Fig. 7B) are extracted from the wide line ^{2}H NMR spectrum and presented separately. In the center band (Fig. 7A) one clearly observes a high (H), middle (M), and low (L) frequency peaks at 13, 3, and 0 ppm. In the high frequency side band (Fig. 7B) one observes the prominent high frequency peak with significantly diminished intensity for the middle and low frequency peaks. The quadrupolar line shapes are obtained by plotting the

intensities of the H, M, and L peaks for each side band (Fig. 7C). There are two important pieces of information in Fig. 7C. First, the total area of the high frequency peak is far greater than that of the middle and low frequency peaks, further confirming what is observed in the rotor synchronized isotropic ^{2}H NMR spectra. Second, in the case of the high frequency peak (H) one observes a classic, albeit broadened, double peaked Pake powder pattern (Fig. 7C) consistent with deuterium in a rigid environment. The frequency spread between the pair of peaks is indicative of a C_q of ca. 110 KHz. This magnitude of C_q is consistent with an immobile deuteron in a site with an O-D•••O distance that would yield a corresonding ^{1}H NMR frequency of ca. 16 ppm (Eckert et al. 1987, Eckert et al. 1988, Xue and Kanzaki 2001). In the case of the middle and low frequency peaks, however, one observes a very different quadrupolar line shape, each with a single maxima centered near 0 frequency. Such line shapes are typical of partial motional (dynamical) averaging of the ^{2}H quadrupolar interaction, e.g., through O-D wagging or flipping motion (Eckert et al. 1987, Schmidt-Rohr and Speiss 1994). Such motional averaging leads to considerable reduction in the ^{2}H spectral width and greatly reduces concerns of off-resonance effects, i.e., where as the worse case scenario predicts a potential 8 % intensity artifact (see discussion above) assuming rigid deuterons, the observation that the deuterons in the low frequency sites are not rigid further reduces any potential artifact related to off-resonance effects.

^{1}H and ^{2}H MAS NMR of model basalt composition glass

The large intramolecular partitioning of H and D is readily observed in Figs 1-6 because of the relatively simple structure of NS4 glass. An important question is whether intramolecular hydrogen isotope partitioning would also occur in glasses and melts with more geochemically relevant compositions. To test this, a quenched silicate melt designed to model basaltic melt composed of Ca, Na, Mg, Al, Si oxides (CNMAS) was synthesized with 6 wt % water D:H 1:1. The ^{1}H and ^{2}H solid state NMR spectra of the CNMAS glass quenched from melt are presented (overlayed) in fig. 8. Significant differences in deuteron and proton speciation are evident. There is much more electronic diversity in the CNMAS glass compared with the NS4 glass leading to a more complex NMR spectrum. Notwithstanding the resulting increased spectral complexity, the ^{1}H and ^{2}H NMR spectra are quite different indicating preferential affinity of deuterons and protons for different molecular sites within the hydrous model basalt structure of the CNMAS glass. As in the case of the simpler hydrated NS4 glass, ^{2}H prefers sites with shorter O-D•••O distances, hence higher NMR frequency.

Discussion

Given that these glasses are synthesized and quenched at such high temperatures classical equilibrum fractionation, i.e., due to differences in zero-point energies (Bigeleisen and Mayer 1947; Urey 1947), is not expected. A lack of any spectroscopic evidence of broadening of OH stretching vibrations at 500 to 600 °C would appear to rule out isotope fractionation associated with hydrogen bonding effects (Mysen 2010).

413 The fact that ^2H prefers sites with shorter O-D•••O distances suggests deuterium favors
414 sites with small molar volume and the observed large intramolecular partitioning is
415 likely derived from density or molar volume isotope effects (e.g. Driessner 1997; Horita
416 et al. 2002; Polyakov et al. 2006). Molar volume isotope effects (MVIE) have been
417 invoked to explain a pressure-dependence of isotopic fractionation between water and
418 $Mg(OH)_2$, attributed to differences in the molar volume of D_2O and H_2O (Horita et al.
419 2002). Also, recent high pressure neutron diffraction experiments on $Mg(OD)_2$ indicate
420 greater compressibility than $Mg(OH)_2$ (Horita et al. 2010). For supercritical fluids at
421 elevated pressures, theoretical calculations and experimental studies have supported the
422 significant effect of D_2O and H_2O molar volume differences on isotope exchange
423 reactions between D-H bearing dissolved volatiles (Polyakov et al. 2006; Foustoukos
424 and Mysen 2012, 2013).

425 Molar volume isotope effects have been identified in aqueous ionic solutions
426 containing sodium acetate and sodium hydroxide, where at elevated temperatures and
427 pressures (up to the critical point of aqueous solutions) the Na^+ solvation volume with
428 D_2O differs significantly than that with H_2O (Tevani et al. 2007; Erikson et al. 2011). In
429 NS4 glasses, the extent to which water and Si-OH solvate Na^+ is equivocal (Zotov et al.
430 1996). Solvation isotope effects in aqueous solutions are predicted to diminish as
431 temperature increases (Driesner and Seward 2000). How increased pressure might
432 change such effects is not known.

433 The NS4 glasses in the present study were synthesized from silicate melts at
434 1400 °C and 1.5 GPa (corresponding to a depth of 50 km). The partial molar volume of
435 water in quenched silicate melts is low, ca. 12 cm^3/mol (Richet et al. 2000). This is far

436 denser than pure water at the same conditions, suggesting that partial molar volume
437 isotope effects may be expected (Driessner 1997; Horita et al. 2002; Palyakov et al.
438 2006). The O-H•••O distances for the high freqency and low frequency sites correspond
439 to 2.47 Å and 2.9 Å, respectively (Eckert et al. 1988, Xue and Kanzaki 2001); in terms
440 of molar volume this could imply that the high frequency site has a molar volume that is
441 60 % that of the low freqency site. This is consistent with deuterons in the high
442 frequency site being rigid (immobile), whereas the deuterons in the low to medium
443 frequency sites are at least partially mobile (Fig. 7). Such a large molar volume
444 difference evidently has a strong influence on the affinity of H and D for different sites
445 within NS4 melt quenched to glass (Fig. 1-8).
446
447 **Implications**
448 The fact that deuterons and protons have different affinities for different
449 molecular sites in glasses and presumably melts based on molar volume differences
450 potentially has important implications for understanding Earth's deep hydrological cycle
451 as well as the D/H compostion of Earth's first oceans and mantle. For example, during
452 the magma ocean phase of Earth's earliest history, shortly after accretion and, again,
453 following the moon forming impact, much if not all of the Earth was molten.
454 Devolatilization during crystallization of the magma ocean might have contributed the
455 water from which Earth's oceans ultimately formed (Drake and Righter 2002). Although
456 the solubility of water in silicate melts at high pressure is relatively high (Richet et al.
457 2000), eventually during crystallization the water content will saturate the melt leading
458 to exsolution of a silica saturated aqueous phase coexisting with the water-saturated

459 melt. Neither the cation-silicate ratio or NBO/T of silicate is expected to be the same for
460 co-existing melt and silica saturated aqueous fluid (Mysen 2010, 2013), therefore
461 significant D-H isotope partitioning between melt and aqueous fluid could be expected.
462 Furthermore, it has been noted that complete extraction of volatiles from melt from a
463 deep magma ocean even under moderate extents of crystallization becomes physically
464 difficult and perhaps impossible (Elkins-Tanton 2011); implying that some water must
465 have been retained in the mantle even after degassing that may have formed the Earth's
466 oceans.

467 In model hydrated NS4 melts saturated with water is has been shown that
468 $D/H_{Water\text{-}Melt} \neq D/H_{Water\text{-}fluid}$ (Mysen 2013). In effect, the D/H isotope exchange between
469 silicate melts and fluids appears to be controlled mainly by the solubility and speciation
470 of silicate species dissolved in the fluid phase. The present study provides further
471 evidence that D-H partitioning between molecular and structural water is independent of
472 the water content in the silicate melt, but largely constrained by the affinity of deuterium
473 into sites with lower molar volume. While it is not possible at this stage to predict the
474 magnitude or even the direction of D-H partitioning between fluid and melt during
475 magma ocean crystallization for geochemically realistic hydrous melt compositions,
476 these experimental data strongly suggest such an isotope partitioning process governed
477 by different intermolecular site affinities of H and D in fluids and melts must be
478 considered a distinct possibility early in Earth's history.
479

Acknowledgments

This research was conducted with support from a NASA Astrobiology Institute awarded to the Carnegie Institution of Washington and NSF-EAR-1250499 (DF, BM, GC). All NMR data were acquired using the W. M. Keck Solid State NMR facility supported in part by the W. M. Keck Foundation, the NSF, and the Carnegie Institution of Washington.

References

Ashbrook S. E. and Wimperis S. (2005) Rotor-synchronized acquisition of quadrupolar satellite transition spectra: practical aspects and double-quantum filtration. Journal of Magnetic Resonance. 177, 44-55.

Bak M., Rasmussen J. T., and Nielsen N. C. (2000) SIMPSON: A general simulation program for Solid-State NMR spectroscopy. Journal of Magnetic Resonance 147, 296-330.

Bell D. R. and Ihinger P. D. (2000) The isotopic composition of hydrogen in nominally anhydrous mantle minerals. Geochimica et Cosmochimica Acta 64, 2109-2118.

Bigeleisen J. and Mayer M. G. (1947) Calculation of equilibrium constants for isotopic exhange reactions. Journal of Chemical Physics. 15, 261-267.

Cody G. D., Mysen B. O., and Lee S. K. (2005) Structure vs. composition: a solid state ^{1}H and ^{29}Si NMR study of quenched glasses along the Na_2O-SiO_2-H_2O join. Geochimica et Cosmochimica Acta 69, 2373-2384.

Dobson P. F., Epstein S., and Stolper E. M. (1989) Hydrogen Isotope fractionation between coexisting vapor and silicate glasses and melts at low pressure. Geochimica et Cosmochimica Acta 53, 2723-2730.

Drake M. J. and Righter K. (2002) Determining the composition of the Earth. Nature 416, 39-44.

Driesner T. (1997) The effect of pressure on Deuterium-Hydrogen Fractionation in High-temperature water. Science 277, 791-794.

Driessner T. and Seward T. M. (2000) Experimental and simulation study of salt effects and pressure/density effects on oxygen and hydrogen stable isotope liquid-vapor fractionation for 4-5 molal aqueous NaCl and KCl solutions to 400 °C. Geochimica et Cosmochimica Acta. 64, 1773-1784.

Eckert H., Yesinowski J. P., Stolper E. M., Stanton T. R., and Holloway J. (1987) The state of water in rhyolitic glasses. A deuterium NMR study. Journal of. Noncrystalline Solids. 93, 93-114.

Eckert H., Yesinoski J. P., Silver L. A., and Stolper E. M. (1988) Water in silicate glasses: quantitation and structural studies by ^{1}H solid echo and MAS-NMR methods. Journal of Physical Chemistry. 92, 2055-2064.

Eckman R. R. (1982) Hydrogen and Deuterium NMR of solids by Magic Angle Spinning. Thesis, University of California, Berkeley. 231p.

Elkins-Tanton L. T. (2011) Magma oceans in the inner Solar System. Annual Reviews in Earth and Planetary Sciences 40, 113-139.

Erikson K. M., Arcis H., Raffa D., Zimmerman G. H. and Tremaine P. R. (2011) Deuterium isotope effects on the ionizationo constant of acetic acid in H_2O and D_2O by AC conductance from 368 to 548 K at 20 MPa. Journal of Physical Chemistry B, 115, 3038-3051.

Ernst R. R., Bodenhausen G., and Wokaun A. (1991) Principles of NMR in One and Two Dimensions, Clarendon Press, Oxford. 610p.

Foustoukos D. I. and Mysen B. O. (2012) D/H isotopic fractionation in the H2-H2O system at supercritical water conditions: composition and hydrogen bonding effects. Geochimica et Cosmochimica Acta 86, 88-102.

Foustoukos D. I. and Mysen B. O. (2013) H/D methane isotopologues dissolved in mgmatic fluids: stable hydrogen isotope fractionations in the Earth's interior. American Mineralogist 98, 946-954.

Horita J., Cole D. R., Polyakov V. B. and Driesner T. (2002) Experimental and theoretical study of pressure effects on hydrogen isotope fractionation in the system brucite-water at elevated pressure. Geochimica et Cosmochimica Acta 66, 3769 -3788

Horita J., dos Santos A. M. , Tulk C. A., Chakoumakos B. C. and Palyakov V. B. (2010) High-pressure neutron diffraction study on H-D isotope effects in brucite. Physical Chemistry of Minerals 37, 741-749.

Kohn S. C., Dupree R., and Smith M. E. (1989) Proton environments and hydrogen bonding in hydrous silicate glasses from proton NMR. Nature 337, 539-541.

Kümmerlin J., Merwin L. H., Sebald A., and Keppler H. (1992) Structural role of H_2O in sodium silicate glasses: Results from ^{29}Si and ^{1}H spectroscopy. Journal of Physical Chemistry, 96, 6405-6410.

Kuroda Y., Hariya Y., Suzuoki T., and Matsuo S. (1982) D/H fractionation between water and melts of quartz, K-feldspar, albite and anorthite at high temperature and pressure. Geochemical Journal, 16, 73-78.

Maekawa H., Maekawa T., Kawamura K., and Yokokawa T. (1992) The structural groups of alkali silicate glasses determined from ^{29}Si MAS-NMR. Journal of Non-Crystalline Solids 127, 53-64.

Mysen B. O. (2010) Structure of H_2O-saturated peralkaline melt and coexisting aluminosilicate saturated fluid determined in-situ to 800 °C and 800 MPa. Geochimica et Cosmochimica Acta, 74, 4123-4139.

Mysen B. O. (2013) Hydrogen isotope fractionation between coexisting hydrous melt and silicate-saturated aqueous fluid: An experimental study in situ at high pressure and temperature. American Mineralogist. 98, 376-387.

Mysen B. O. and Richet P. (2005) *Silicate Glasses and Melts* Elsevier, New York. 544p.

Nowak M. and Behrens H. (1995) The speciation of water in haplogranitic glasses and meltsby in-situ near-infrared spectroscopy. Geochimica et Cosmochimica Acta. 59, 3445.

Pineau F., Shilobreeva S. , Kadik A., and Javoy M. (1998) Water Solubility and D/H fractionation in the system basalitc andesite – H_2O at 1250 ° and between 0.5 an 3 kbars. Chemical Geology. 147**,** 173-184.

Polykov V. B., Horita J. and Cole D. R. (2006) Pressure effects on the reduced partition function ratio for hydrogen isotopes in water. Geochimica et Cosmochimica Acta **70**, 1904-1913.

Richet P., Roux J. and Pineau. F. (1986) Hydrogen isotope fractionation in the system H_2O-liquid $NaAlSi_3O_8$: new data and comments on D/H fractionation in hydrothermal experiments. Earth and Planetary Science Letters. 78, 115-120.

Richet P., Whittington A., Holtz F., Behrens H., Ohlhorst S., and Wilke M. (2000) Water and density of silicate glasses. Contributions in Mineralogy and Petrology. **138**, 337-347.

Schaller T. and Sebald A. (1995) One- and two-dimensional ^{1}H magic angle spinning experiments on hydrous silicate glasses. Solid State Nuclear Magnetic Resonance 5, 89-102.

Schmidt-Rohr K. and Spiess H. W. (1994) Multidimensional Solid-State NMR and Polymers. Academic Press, New York. 478p.

Stolper E. M. (1982) Water in silicate glasses. An infrared spectroscopic study. Contributions in Mineralogy and Petrology. 81, 1-17.

Urey H.C. (1947) The thermodyamic properties of isotopic substances. Journal of the Chemical Society (London) 5, 562-581.

Tevani L. N., Balodis E. C., and Tremaine P. R. (2007) Apparent and standard partial molar volumes of NaCl, NaOH, and HCl in water and heavy water at T=523 and 573 K at p= 14 MPa. Journal of Physical Chemistry B 111, 2015-2024.

Xue X. and Kanzaki M. (2001) An Ab-initio calculation of ^{17}O and ^{1}H NMR parameters for various OH groups: Implications to the speciation and dynamics of dissolved water in silicate glasses. Journal of Physical Chemistry. B. 105, 3422-3434.

Xue X. and Kanzaki M. (2009) Proton distribution and hydrogen bonding in crystalline and glassy hydrous silicates and related inorganic materials: insights from high-resolution Solid State NMR Spectroscopy. Journal of the American Ceramic Society 92, 2803-2830.

Zotov N., Keppler H., Hannon A. C. and Soper A. K. (1996) The effect of water on the structure of silicate glasses- a neutron diffraction study. Journal of Noncrystalline Solids 202, 153-163.

Zotov N. and Keppler H. (1998) The influence of water on the structure of hydrous sodium tetrasilicate glasses. American Mineralogist 83, 823-834.

Figure Captions

Figure 1. *Left*, solid state ^{29}Si MAS-NMR spectra of hydrated sodium tetrasilicate melt quenched to glass with 9 wt % water, variously deuterated from 100 %, 90 % and 0 %. Dashed lines highlight the silicate Q species, where for Q^n, n=the number of bridging oxygens: Q^4 (-103 ppm), Q^3 (-95 ppm), Q^2 (-90 ppm). These ^{29}Si MAS-NMR spectra are statistically indistinguishable and reveal that D and H depolymerize the glass network similarly. *Center*, solid state ^{1}H MAS-NMR spectra of hydrated NS4 glass (Center-Top)

(9 wt% water, 90 % D 10 % H), gypsum (Center-Middle), and hydrated SiO_2 glass (Center-Bottom). *Right*, solid state ^2H NMR spectra of deuterated NS4 glass (Right-Top) and deutrated SiO_2 glass (Right-Bottom).

Figure 2: ^1H (left) and ^2H NMR spectra of hydrated NS4 glasses with 3 wt. % water with varying D-H content.

Figure 3: ^1H (left) and ^2H NMR spectra of hydrated NS4 glasses with 6 wt. % water with varying D-H content.

Figure 4: ^1H (left) and ^2H NMR (right) spectra of hydrated NS4 glasses with 9 wt. % water with varying D-H content.

Figure 5: Quantitative analysis of D-H speciation in hydrated silicate melts quenched to glass with variation in total water content (3, 6 and 9 wt %) and D-H content of the water. High frequency (black) vs. low frequency (gray) abundances between ^1H and ^2H solid state NMR are different (bottom and middle). The partitioning ratio, R, between water in high frequency and low frequency environments is very large (R=3.1) (top).

Figure 6: ^1H (left) and ^2H NMR (right) spectra of hydrated NS4 glasses with 6.3 wt. % water with D:H of the water being 50:50 synthesized at 1400 °C, 1.5 GPa for 48 hours, quenched to glass at a rate of 1 °C/sec. Large intramolecular partitioning is still observed (R=3.1)

671

672 **Figure 7:** Wide line ^{2}H NMR spectrum of hydrated NS4 glass (9 wt % D_2O). **A**) The
673 central band highlighting the high (H), medium (M), and low (L) frequency deuterium
674 resonances. **B**) The forth (most intense) high frequency side band- note the diminished
675 intensity of the M and L peaks. **C**) ^{2}H quadrupolar line shapes for the H, M, and L
676 deuterium resonances. Note that the high frequency peak exhibits a broadened classic
677 Pake powder pattern indicative of deuterium in a rigid environment. The M and L
678 powder patterns exhibit the characteristics of deuterons in more mobile environments,
679 e.g., O-D wagging motion.

680

681 **Figure 8**: ^{1}H (black) and ^{2}H (gray) solid state NMR spectra of a hydrated Ca, Mg, Na,
682 Al, Si oxide glass (a model basalt composition without Fe) with 6 wt % water (D:H 1:1).
683 The lack of fine structure relative to the NS4 glasses is due to a much larger number of
684 electronic environments available for H and D to reside with the glass structure. It is
685 evident that large intramolecular D-H partitioning exists, where D tends to favor
686 environments corresponding to the high frequency (shorter O-[H,D]•••O distance)
687 resonances and H favors environments corresponding to the lower frequency (longer O-
688 [H,D]•••O distance) resonances.

689

690

691

692

693

694

695

Table 1

Total water content and $^{2}H:^{1}H$ concentration of the synthesized glasses

Composition of anhydrous glass	**total water content** (wt %)	(mol %)	**$^{2}H/^{1}H$**	**H content** (mol %)	**D content** (mol %)	**run duration** (hrs)
NS4	3.3	11.4	100 : 0	22.8	0	3
NS4	3.3	11.4	90 : 10	2.2	20.6	3
NS4	3.1	11.1	50 : 50	11.0	11.0	3
NS4	6.3	21.1	50 : 50	21.0	21.0	3, 48
NS4	6.3	21.1	90 : 10	4.2	38.0	3
NS4	6.3	21.1	0 : 100	42.2	0	3
NS4	9.9	29.4	100 : 0	0	58.8	3
NS4	9.9	29.4	90 : 10	5.8	52.8	3
NS4	9.4	29.2	50 : 50	29.2	29.2	3
NS4	9.0	29.2	0 : 100	58.4	0	3
CMNAS	6.3	31.4	50 : 50	31.4	31.4	3

Table 2

^{29}Si NMR Q-species determination and water speciation OH to H_2O calculations

Run no.	D:H (9 wt % water)	Integration %(Hi, Mid, Low)	NBO/T	% as H_2O	% as Si-OH
6881	100% H	21.9 (-90 ppm) Q2		49.0	51.0
		46.7 (-95 ppm) Q3	0.91		
		31.4 (-103 ppm) Q4			
6872	9:1	21.2 (-90 ppm) Q2		43.5	56.5
		49.9 (-95 ppm) Q3	0.92		
		28.8 (-103 ppm) Q4			
6879	100% D	20.7 (-90 ppm) Q2		48.7	51.3
		46.7 (-95 ppm) Q3	0.88		
		32.7 (-103 ppm) Q4			

742

743

744

745

746

747

748

749

750
751
752
753

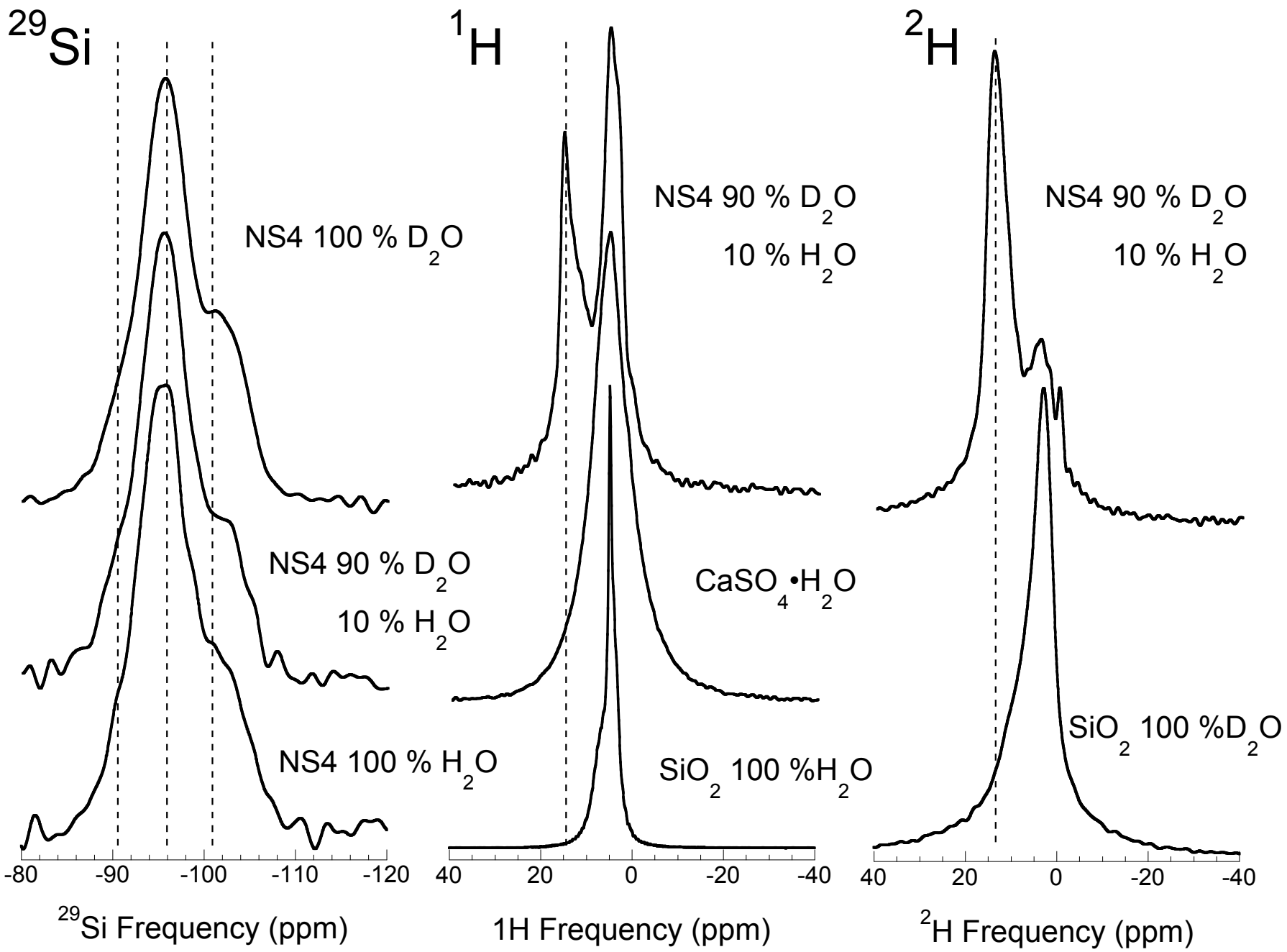
29Si
1H
2H
NS4 100 % D2O
NS4 90 % D2O
10 % H2O
NS4 100 % H2O
CaSO4•H2O
SiO2 100 %H2O
SiO2 100 %D2O
-80
-90
-100
-110
-120
40
20
0
-20
-40
29Si Frequency (ppm)
1H Frequency (ppm)
2H Frequency (ppm)

Figure 1

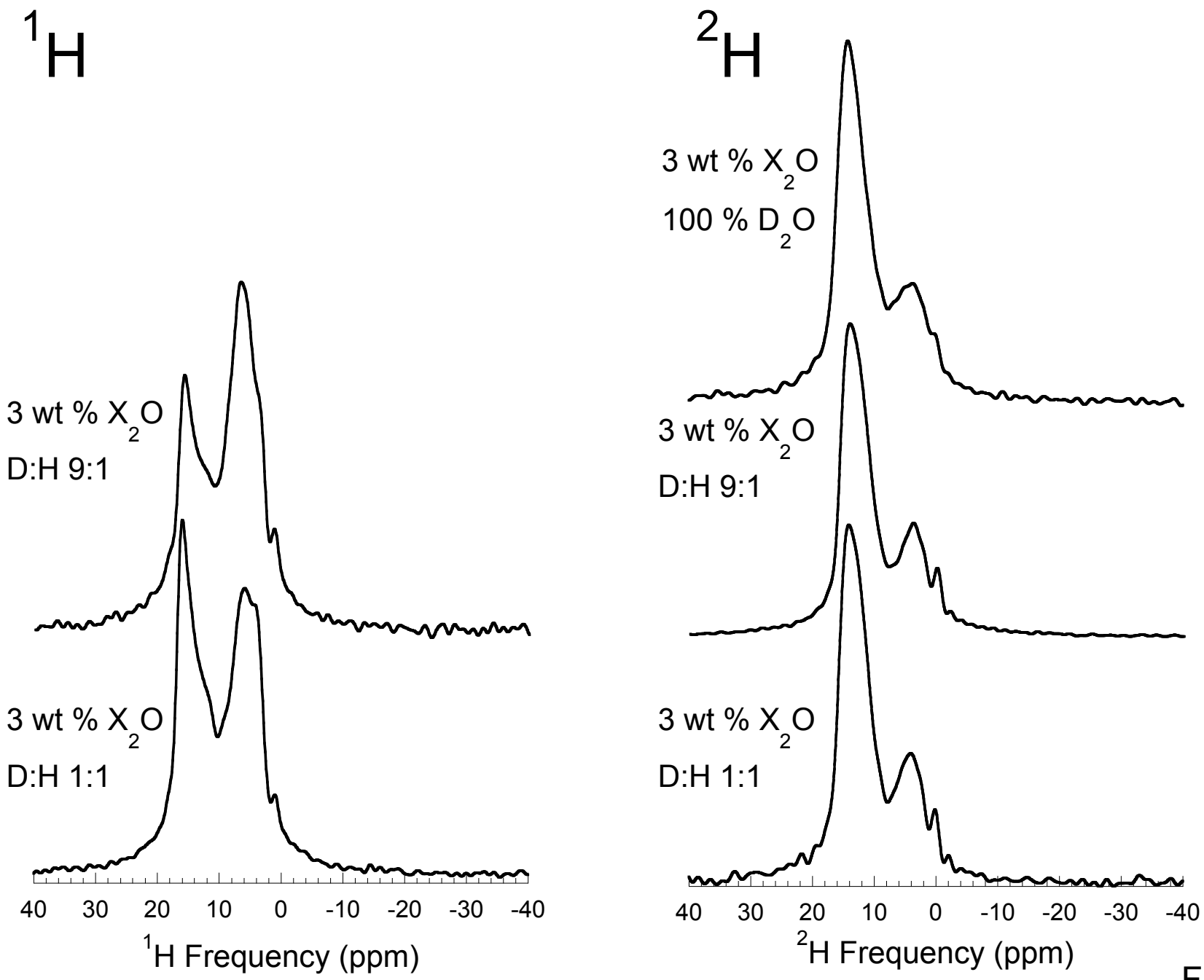
^{1}H
3 wt % X_2O
D:H 9:1
3 wt % X_2O
D:H 1:1
40 30 20 10 0 -10 -20 -30 -40
^{1}H Frequency (ppm)
^{2}H
3 wt % X_2O
100 % D_2O
3 wt % X_2O
D:H 9:1
3 wt % X_2O
D:H 1:1
40 30 20 10 0 -10 -20 -30 -40
^{2}H Frequency (ppm)

Figure 2

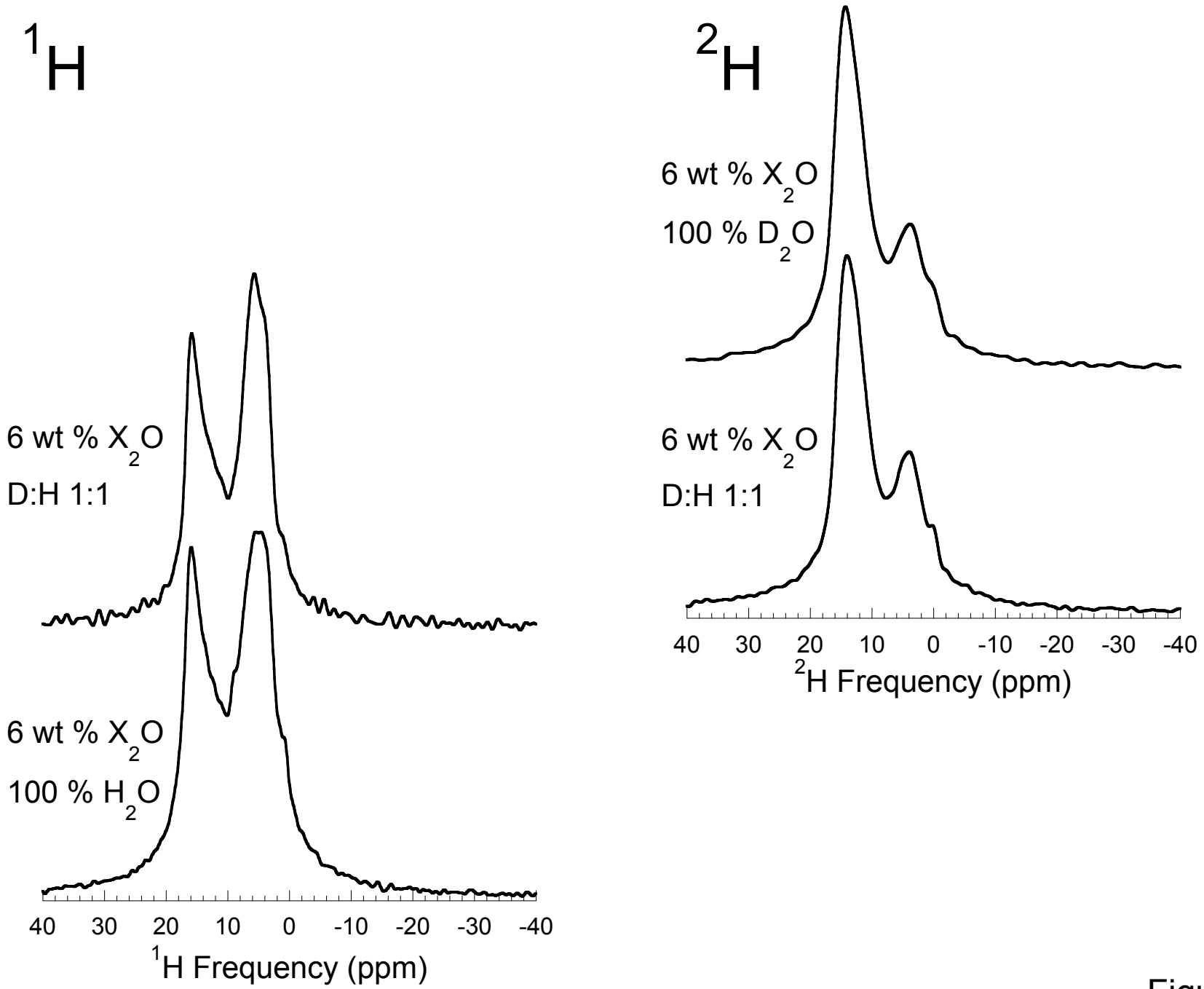
^{1}H
6 wt % X_2O
D:H 1:1
6 wt % X_2O
100 % H_2O
40 30 20 10 0 -10 -20 -30 -40
^{1}H Frequency (ppm)
^{2}H
6 wt % X_2O
100 % D_2O
6 wt % X_2O
D:H 1:1
40 30 20 10 0 -10 -20 -30 -40
^{2}H Frequency (ppm)

Figure 3

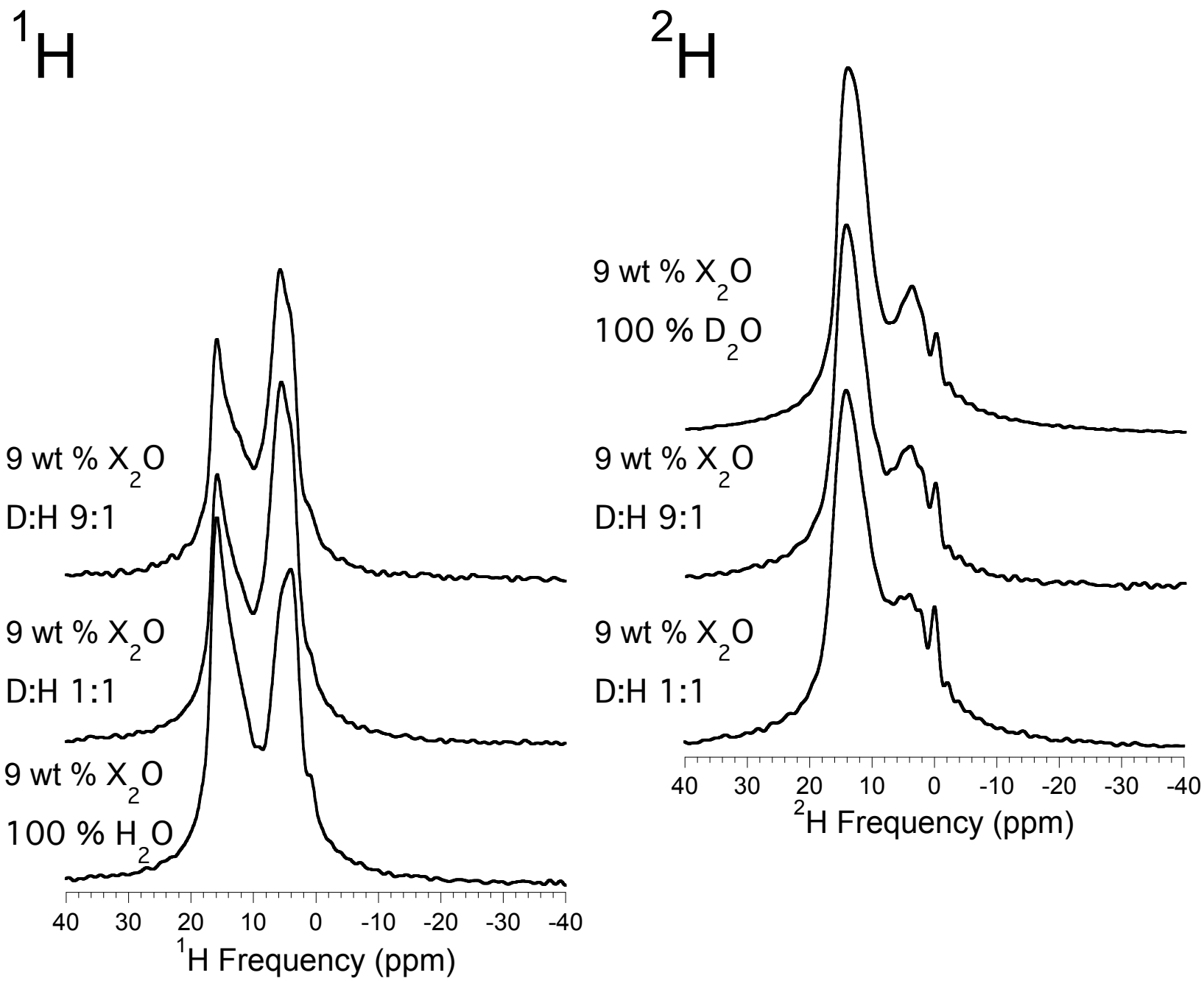
^{1}H
9 wt % X_2O
D:H 9:1
9 wt % X_2O
D:H 1:1
9 wt % X_2O
100 % H_2O
40 30 20 10 0 -10 -20 -30 -40
^{1}H Frequency (ppm)
^{2}H
9 wt % X_2O
100 % D_2O
9 wt % X_2O
D:H 9:1
9 wt % X_2O
D:H 1:1
40 30 20 10 0 -10 -20 -30 -40
^{2}H Frequency (ppm)

Figure 4

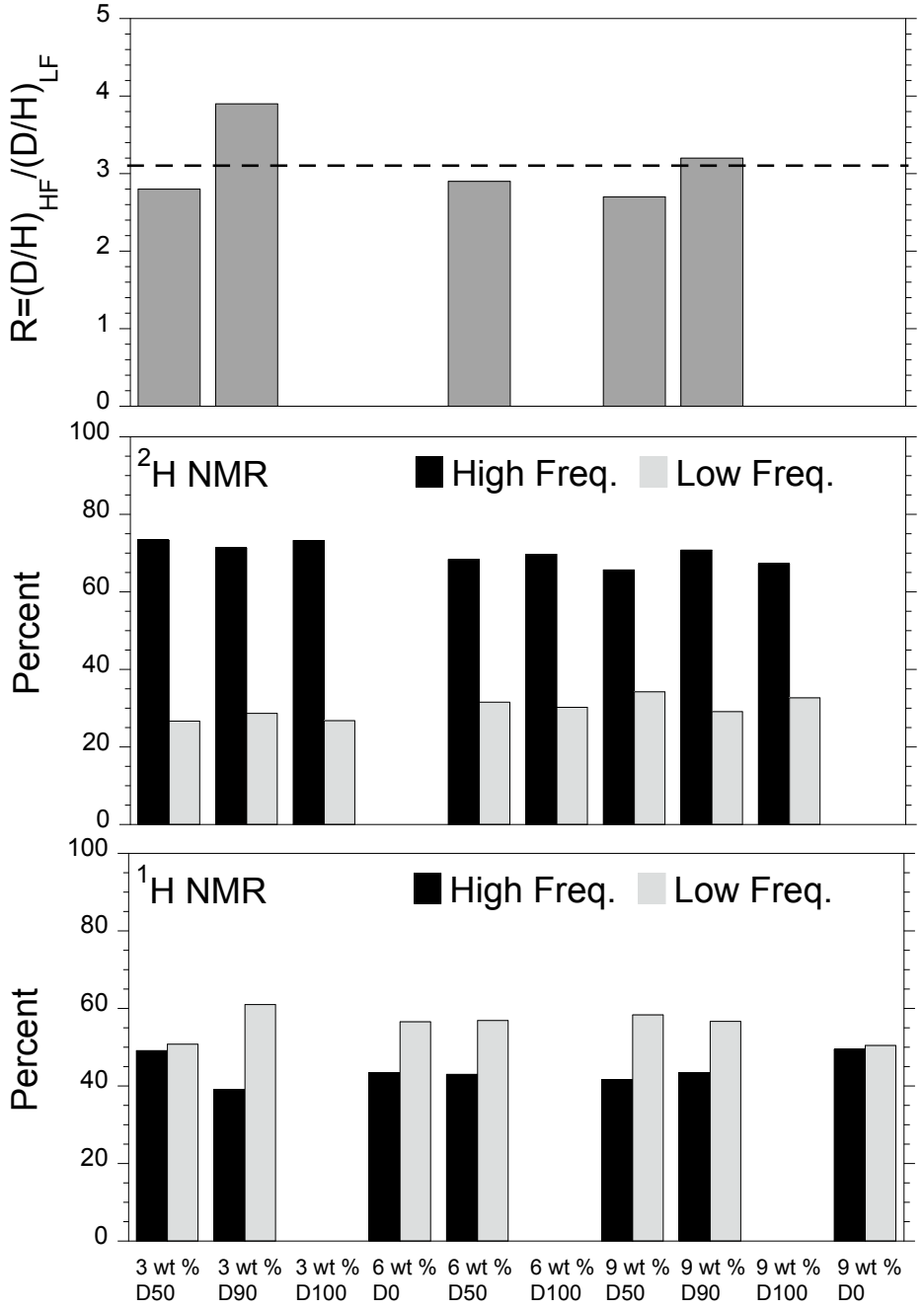
R=(D/H)HF/(D/H)LF
5
4
3
2
1
0
2H NMR
High Freq.
Low Freq.
Percent
100
80
60
40
20
0
1H NMR
High Freq.
Low Freq.
Percent
100
80
60
40
20
0
3 wt % D50
3 wt % D90
3 wt % D100
6 wt % D0
6 wt % D50
6 wt % D100
9 wt % D50
9 wt % D90
9 wt % D100
9 wt % D0

Figure 5

^{1}H NMR

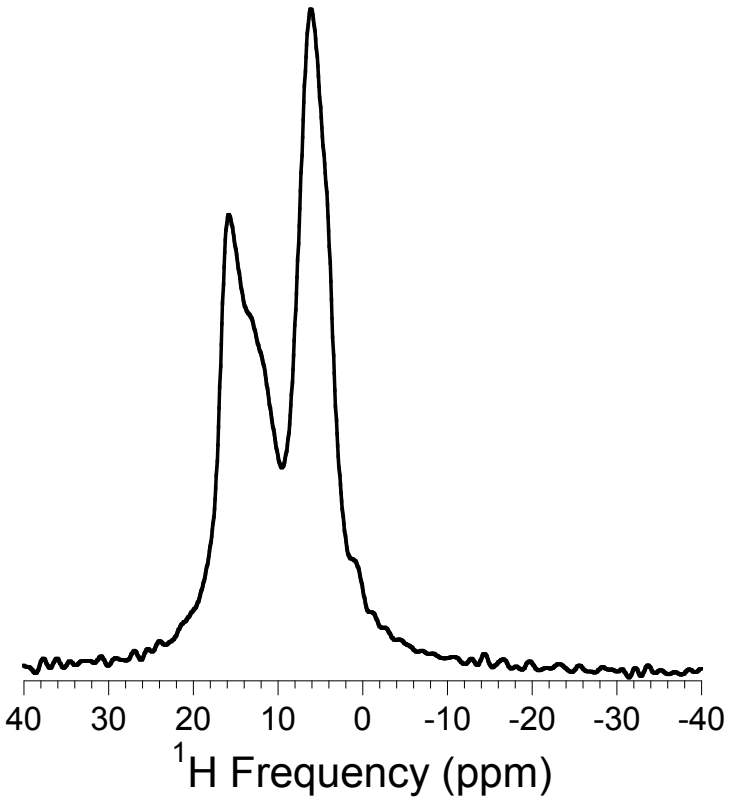

^{2}H NMR

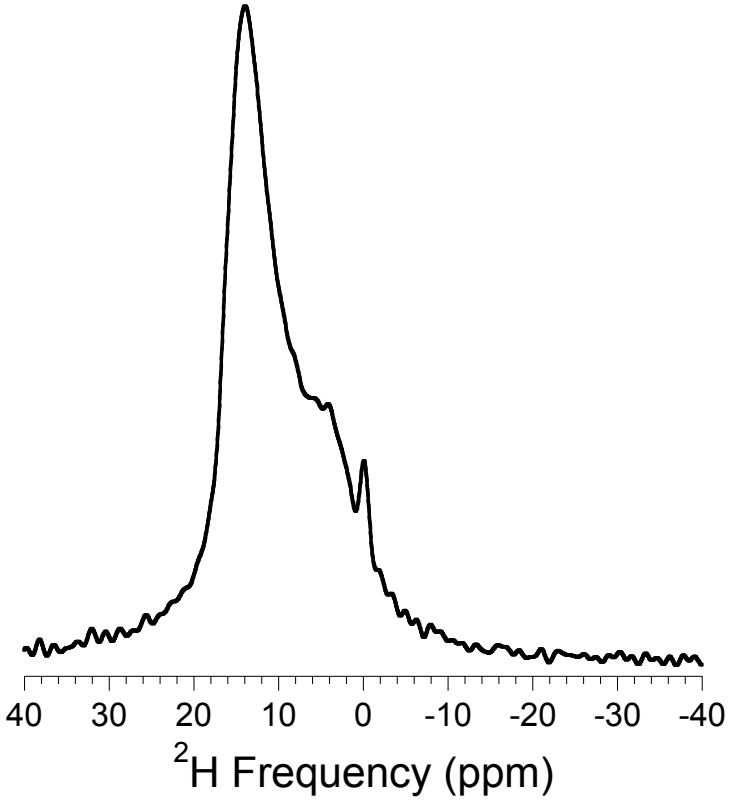

Figure 6

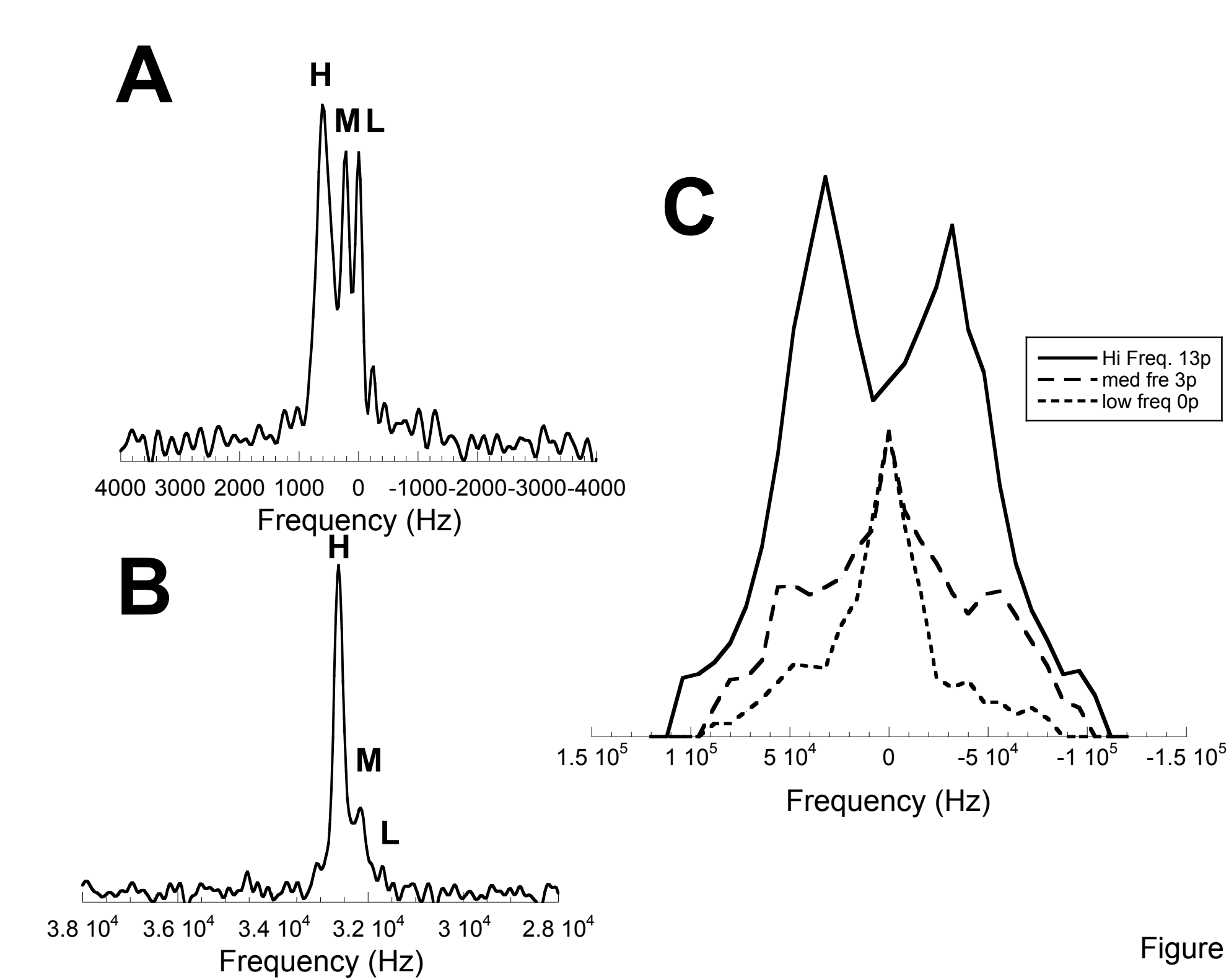
A
H
M L
4000 3000 2000 1000 0 -1000-2000-3000-4000
Frequency (Hz)
B
H
M
L
3.8 10^4 3.6 10^4 3.4 10^4 3.2 10^4 3 10^4 2.8 10^4
Frequency (Hz)
C
Hi Freq. 13p
med fre 3p
low freq 0p
1.5 10^5 1 10^5 5 10^4 0 -5 10^4 -1 10^5 -1.5 10^5
Frequency (Hz)

Figure 7

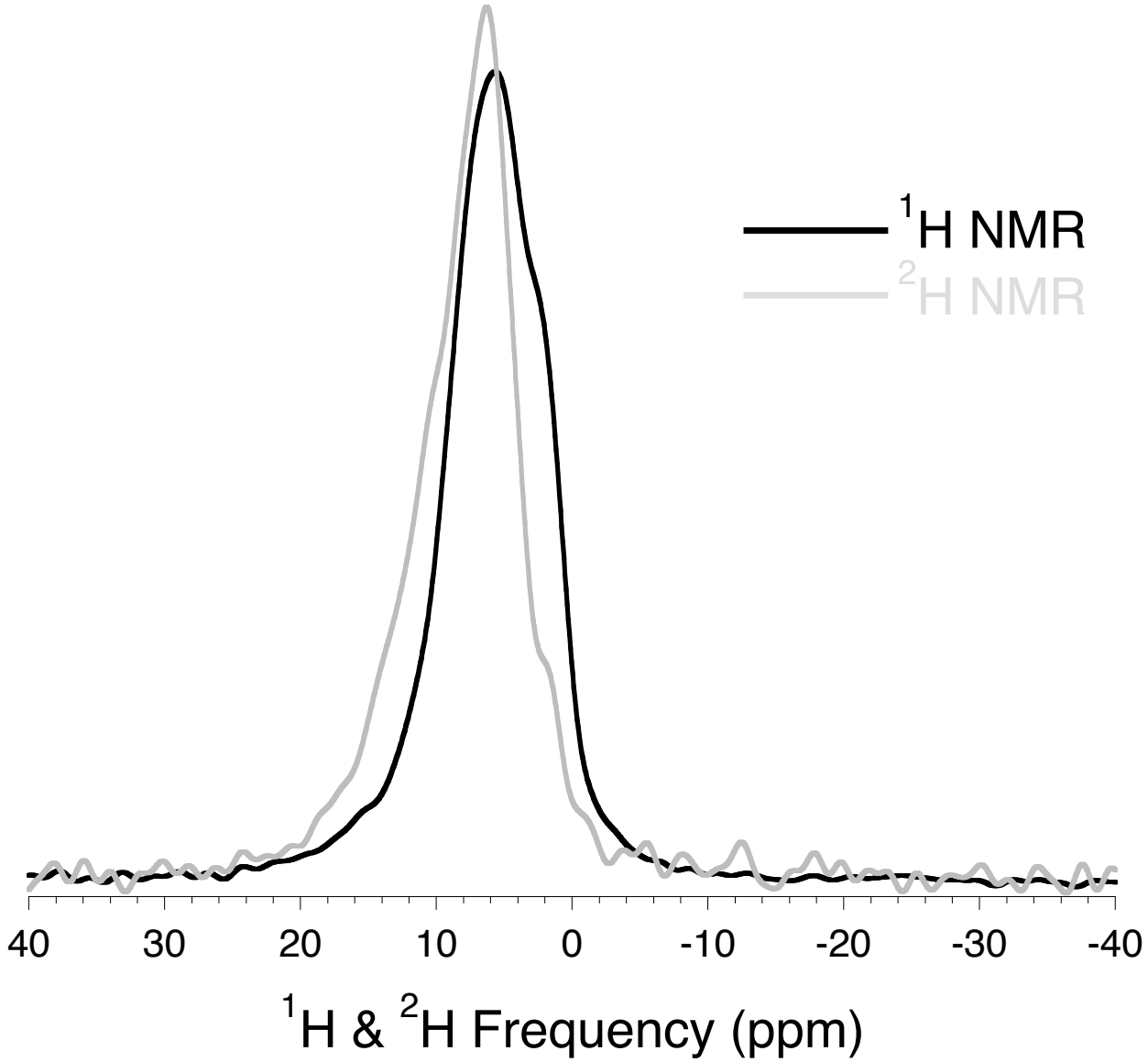

Figure 8